Indian Geotech J (February 2019) 49(1):70–89
https://doi.org/10.1007/s40098-017-0283-1

ORIGINAL PAPER

Seepage and Stability Analysis of Durgawati Earthen Dam: A Case Study

N. Himanshu[1] · **A. Burman**[1]

Received: 3 February 2017 / Accepted: 19 October 2017 / Published online: 30 October 2017
© Indian Geotechnical Society 2017

Abstract Analysis of dam slopes is of much importance because its failure may prompt loss of lives and properties. In this paper, both seepage and slope stability analyses of the earthen embankment dam of Durgawati reservoir project in the region of Kaimur–Bihar is presented. The analyses are performed using geotechnical software GEOSTUDIO 2007 (SEEP/W in Seepage analyses, Software permitted for limited period of use by GeoSlope Office, Canada, 2007; SLOPE/W in Stability Analysis, Users guide version 5, GeoSlope Office, Canada, 2002). Two sections of the Durgawati reservoir project have been considered for detailed stability analysis namely one from RD 640.09 m CH 21.00 and another from RD 670.57 m CH 22.00. Both upstream and downstream slopes, located at the dam site have been investigated for long-term stability for full reservoir condition (i.e. steady-state seepage) and drawdown condition (i.e. transient-state). It has been observed that the Factor of safety against slope failure at the upstream face is substantially greater than that of the downstream slope because of resisting effect of the reservoir water on the upstream slope. The stability of the upstream slope of the dam decreased considerably during drawdown condition. The structure lies in the earthquake prone area Zone III as per IS 1893-2002. Therefore, a pseudo-static analysis has been performed using different horizontal earthquake coefficient in combination with both steady-state as well as transient-state seepage condition.

✉ A. Burman
avijitburman@yahoo.com

[1] Department of Civil Engineering, Geo-Technical Engineering, NIT Patna, Bihar, India

Keywords Slope stability analysis · Limit equilibrium method · Bishop's simplified method · Durgawati earthen embankment · Steady state seepage analysis · Transient seepage analysis · Pseudo static seismic analysis

Introduction

An earthen embankment dam is a structure with a complex geometry and expected to remain stable under all conditions. Stability related issues of built in slopes are common challenges to both professional researchers and engineers. Failure of the earthen dam may be caused by change in resulting stress by rainfall, variation in ground water table, sudden change in water level of the reservoir or seismic event, occurring individually or in combination.

In case of earthen dam holding reservoir water, the knowledge of water flow inside embankment is extremely important to estimate the seepage loss inside the water storage dam. In the present study, the quantity of water flowing through the pores of the soil and its influences on the shear strength is of great concern in stability of slopes. To predict the stability of a dam at any stage, a stability analysis under static load for steady-seepage and transient-state seepage has been performed. If the dam is to be constructed in an earthquake prone area, proper analyses should be carried out to assess the stability of structure against seismic loading.

There are several available commercial softwares [1, 2] which incorporate the facilities of both seepage and stability analyses of earthen embankment slopes. The first limit equilibrium method proposed by Fellenius [3] for slope analysis was based on the idea of dividing potential sliding mass into discrete vertical slices for a circular slip surface. Bishop [4, 5] reformulated the method of slice by adding a new inter-slice normal force, and calculated the factor of

safety (FOS) with great precision. At the same time, Janbu [6] developed a simplified method for non-circular failure surfaces. Later, a generalized procedure of slices (GPS) was proposed by Janbu [7] by including inter slice forces. Later, Morgenstern and Price [8], Spencer [9] restructured the method of slice, for non-circular failure as well as for circular failure surface, by including both inter-slice normal forces and inter-slice shear forces satisfying both moment and force equilibrium. In 1973, a new limit equilibrium based technique was devised by Sarma [10] to examine the stability of slope. Several others investigators like Lowe–Karafaith [11] and Corps of Engineers [12] independently proposed a method satisfying only force equilibrium by considering both inter-slice normal as well inter-slice shear force with a difference in assumption for the inter-slice force function. At the University of Saskatchewan, Fredlund and Krahn [13] developed General limit equilibrium (GLE) formulation. These are some popular limit equilibrium based analysis methods for assessing the stability of earthen slope being used in geotechnical engineering for many years.

Griffiths and Lane [14] proposed advanced numerical methods for stability analysis based on strength reduction technique in combination with finite element method. In addition, Lane and Griffiths [15], Griffiths and Fenton [16], Zheng et al. [17] developed the stability analysis technique based on finite element method.

In recent years, evolutionary algorithms have been introduced with much acceptability for solving non-linear optimization problems. Genetic algorithm is one of the popular techniques that have been used in the recent years to solve slope stability problem. Goh [18, 19], McCombie and Wilkinson [20], Sabhahit et al. [21], Zolfaghari et al. [22], Bhattacharya and Satish [23] have used genetic algorithm for slope stability analysis. Recently, particle swarm optimization is evolving as a powerful optimization technique for analyzing the stability of slope. Cheng et al. [24], Kumar and Reddy [25] have used the particle swarm optimization based approach for estimating the FOS for earthen slope.

In this paper, the seepage and slope stability analyses of Durgawati earthen dam is presented as a case study. Seepage analyses have been carried out considering steady state condition to find out the pore pressure magnitudes. Also, transient state seepage analyses have been carried out to find the same to simulate the drawdown effect of reservoir water. After that, slope stability analyses have been performed to find out the minimum FOS against slope failure using Geo-Studio software [1, 2]. Sivakugan and Das [26] have validated this software for a number of slope stability problems and advocate the use of this software for solving problems related to slope stability. Furthermore, seismic slope stability analyses have been performed by considering horizontal earthquake coefficient under both steady state and transient state seepage condition.

Methodology and Modelling

Stability analysis of earthen embankment dam can be accomplished by different limit equilibrium methods for concluding the critical failure surface and, associated minimum values of Factor of safety. The following section briefly describes the methodology used for analyzing Durgawati earthen dam in Bihar.

Seepage Analysis

The seepage analysis has been performed to predict pore pressure distributions under full reservoir condition by steady-state seepage analysis and under drawdown condition by transient seepage analysis. The estimate of total quantity of seepage losses through an embankment slopes is based on the difference in elevation of water between the upstream and downstream side of the earthen dam along with the hydraulic conductivity of respective embankment material. According to the Darcy's law, the specific discharge through a saturated soil medium is given by;

$$q = k\,i \tag{1}$$

where q = the specific discharge (i.e. discharge per unit area) through the soil medium, k = the hydraulic conductivity of soil material, i = slope of gross available hydraulic head.

Darcy's law was initially derived to estimate the specific discharge for saturated soil. Later research shows that it can also be applied to estimate the flow of water through unsaturated soil media [27, 28]. The quantity of water flowing through a saturated soil mass as well as the distribution of water pressure can be estimated by the theory of flow of fluids through any porous medium. The general form of two-dimensional differential equation (Laplace equation) to estimate seepage is expressed as:

$$\frac{\partial}{\partial x}\left(k_x \frac{\partial H}{\partial x}\right) + \frac{\partial}{\partial y}\left(k_y \frac{\partial H}{\partial y}\right) + Q = \frac{\partial \theta_w}{\partial t}. \tag{2}$$

There are two basic types of seepage analysis, steady-state seepage to simulate reservoir water under full storage conditions and transient-state seepage to simulate drawdown in the reservoir water. The related mathematical formulation associated with each type is expressed as:

Steady-State Seepage

$$\frac{\partial}{\partial x}\left(k_x \frac{\partial H}{\partial x}\right) + \frac{\partial}{\partial y}\left(k_y \frac{\partial H}{\partial y}\right) + Q = 0. \tag{3}$$

Transient-State Seepage

$$\frac{\partial}{\partial x}\left(k_x \frac{\partial H}{\partial x}\right) + \frac{\partial}{\partial y}\left(k_y \frac{\partial H}{\partial y}\right) + Q = m_w \gamma_w \frac{\partial (H)}{\partial t} \tag{4}$$

where H = total available hydraulic head difference, k_x = the hydraulic conductivity in the horizontal x-direction, θ_w = volumetric water content of the soil, t = time, Q = applied boundary flux i.e. discharge, k_y = the hydraulic conductivity in the vertical y-direction, m_w = the slope of the storage slope, γ_w = the unit weight of water.

Limit Equilibrium Methods for Stability Analysis

Limit equilibrium analysis methods have been used in geotechnical engineering for many years to assess the stability of earthen slopes. An analysis of slope stability starts with supposition that the stability of the slope is governed by downward mobilized forces and upward resisting forces. The relative stability of slope is characterized by the term factor of safety (FOS), defined as the ratio of the summation of shear resistance and shear mobilized for individual slices:

$$FOS = \frac{\sum S_{resistance}}{\sum S_{mobilised}} \tag{5}$$

Shear strength (resistance):

$$S_{resistance} = c' + (N - \mu)\tan\ \phi' \tag{6}$$

Shear stress (mobilized):

$$S_{mobilized} = W \sin\ \alpha \tag{7}$$

where c' = effective cohesion, ϕ' = effective frictional angle, $N = W\cos\ \alpha$ = base normal, W = the slice weight, μ = the pore-water pressure, α = base inclination.

Various limit equilibrium methods viz. Bishop's method [4, 5], Morgenstern and Price [8], Corps of Engineers [12] have been used in the present study.

Pseudo-static Analysis

A seismic pseudo-static analysis represents the earthquake shaking condition by applying an acceleration that creates an inertial force. These forces are in the horizontal directions as well as in vertical directions and act at the center of each slice to exert large influence on the stability of embankment slopes. The forces are defined as:

$$F_h = (a_h W/g) = k_h W \tag{8}$$

$$F_V = (a_v W/g) = k_V W \tag{9}$$

If seismic loading is considered, the $S_{resistance}$ and $S_{mobilized}$ may be determined as follows:

$$S_{resistance} = c' + (N - \mu - F_h \sin\ \alpha)\tan\ \phi' \tag{10}$$

$$S_{mobilized} = W \sin\alpha + F_h \cos\alpha \tag{11}$$

where a_h = horizontal pseudo-static acceleration, a_v = -vertical pseudo-static acceleration, g = gravitational acceleration constant, k_h = horizontal seismic coefficient, k_v = vertical seismic coefficient.

Model Analysis

In this paper, the static and seismic slope stability analyses have been presented for a typical slope section as shown in Fig. 2. The aim of this study is to fulfill three main objectives. The first objective is to find the FOS against slope failure for the Durgawati earthen embankment dam by different limit equilibrium methods under steady-seepage and transient-state seepage. The second objective is to compare the FOS values between the two seepage-states on both downstream as well as upstream slope. Third objective is to find the effect of seismic acceleration on the stability factor of dam slope for both upstream and downstream slopes situated at CH 21.00 and CH 22.00 respectively. Within this framework, the earthen embankment dam has been analyzed for following cases:

Case-1 Static slope stability analysis for downstream and upstream slopes under full reservoir condition (i.e. under Steady-state seepage).

Case-2 Static slope stability analysis for downstream and upstream slopes under drawdown condition (i.e. under transient-state seepage).

Case-3 Pseudo-static earthquake stability analysis, combined with Steady-state seepage using a lateral acceleration of 0.08 g where g is acceleration due to gravity.

Case-4 Pseudo-static earthquake stability analysis, combined with transient-state seepage using a lateral acceleration of 0.08 g where g is acceleration due to gravity.

Case-5 Pseudo-static earthquake stability analysis, combined with Steady-state seepage using a lateral acceleration of 0.16 g where g is acceleration due to gravity.

Case-6 Pseudo-static earthquake stability analysis, combined with transient-state seepage using a lateral acceleration of 0.16 g where g is acceleration due to gravity.

Seepage Analysis

The slopes in the present case study have been evaluated for predicting the ground water flow i.e. to establish the phreatic-line and also the condition of pore-water pressure in the embankment under both Steady-state seepage and transient-state (i.e. Drawdown), using the computer

software SEEP/W. The effect of groundwater flow and seepage has been studied further to evaluate the stability conditions.

Upstream Head Boundary Condition

In this particular problem, the two different boundary conditions have been applied at the interference of the upstream slope and reservoir. It has been used to simulate the field condition of the reservoir water level for seepage analysis.

- **Constant Pressure Head**

In the steady-state seepage analysis, the available head (H) has been specified at the upstream of the embankment as a boundary condition for the initial water level of the reservoir. The available total head is equal to the full storage level. Since, the upstream water level has not changed with time therefore; a constant total head of 128.6 m has been applied for two sections at CH 21.00 and CH 22.00 respectively.

- **Drawdown Pressure Head**

In transient analysis, the water level in the reservoir changes with time; hence the available head (H) specified at the upstream of the embankment is a function of time. A total head versus time function is shown in Fig. 1, which shows the initial and final values of the head. Moreover, the head versus time function represents the total head i.e. when the earthen embankment is under Steady-state seepage, without any reduction in reservoir water level or available head with time and therefore a constant total head of 128.6 m has been applied at time equals to zero. Moreover, to simulate a field drawdown condition, for loss of 19.20 m head in reservoir over a period of 10 days with a final head of 109.4 m, boundary condition has been applied in such a way that the reduction in reservoir water and pore-water pressures in the dam at different time during the whole drawdown process can be modeled. The solution of Eq. (4) subjected to respective boundary condition as shown in Fig. 1 can be found in SEEP/W tutorial [1] as well as in the works by Segerlind [29].

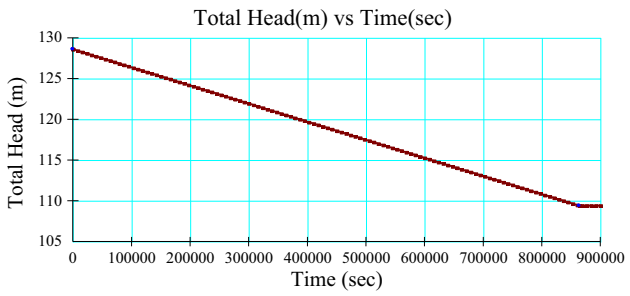

Fig. 1 Head versus time

Stability Analysis

The limit equilibrium based Bishop's method [4, 5] of analysis has been chosen for the slope stability analysis and the computer based software SLOPE/W has been used to obtain the FOS for the two embankment slopes. The slope analysis method suggested by Morgenstern and Price [8] and Corps of Engineers [12] have also been used for analyzing Durgawati earthen dam and their results are presented in tabular form.

Pseudo-Static Analysis

The pseudo-static analyses have been carried out for the slope to study the effects of earthquake shaking by applying horizontal accelerations that produce an inertial force. The Durgawati earthen dam is situated in Zone III as per IS 1893-Part 1 (2002) [30, 31]. The value of horizontal seismic coefficient $k_h = 0.08$ has been considered for the seismic slope stability analysis in Case-3 and Case-4. Hynes-Griffin and Franklin [32] recommended that the pseudo-static acceleration coefficient should be half of the design ground acceleration coefficient which may be treated to be same as the Zone factor as defined in IS 1893-Part 1 (2002) [30, 31]. Also, the value of horizontal seismic coefficient $k_h = 0.16$ is considered for the seismic slope stability analysis in Case-5 and Case-6 which is same as the Zone factor suggested by IS 1893-Part 1 (2002) [30, 31]. The consideration of$k_h = 0.16$ is in agreement with the works of Chakraborty and Choudhury [33] who used a value horizontal seismic coefficient $k_h = 0.10$ for stability analysis of slope in seismic zone II. This value of k_h is same as the zone factor for zone II as per IS 1893-Part 1 (2002) [30, 31].

Durgawati Earthen Dam-Reservoir Project and Model Description

The case study with the relevant slopes has taken up from the Durgawati reservoir project in Kaimur district of the state of Bihar in India. The construction of the earthen embankment dam project started in the year of 1975 and, was complete in the year of 2015. The aim of this project is to irrigate 17,267 ha area of two blocks of Kaimur district and three blocks of Rohtas district. In addition to it, it also aims to provide stabilization of irrigation in (16,200-ha area) due to an old scheme viz. Kudra Weir scheme. The area (16,200 ha) under Kudra Weir has been internalized in the command area of Durgawati reservoir project, and provides gross irrigation of total 33,467-ha area.

The earthen embankment dam of Durgawati reservoir project is 1615.4 m in length and of 46.30 in height. For case study of the Durgawati reservoir project, two slopes are considered for detailed seepage and stability analysis.

One section is from RD 640.09 m at CH 21.00 and another from RD 670.57 m at CH 22.00 respectively. Details of embankment material linked with case study have been listed in Table 1 and the corresponding model of the embankment slopes have been shown in Fig. 2. Moreover, it is evident from the design report that soil used for the construction of earthen embankment is locally available soil. The soil having lower hydraulic conductivity with higher value of cohesion has been used as core material whereas those having higher value of hydraulic conductivity and lower amount of cohesion have been used as shell material.

To obtain the various soil parameter of Durgawati earthen embankment, the water resource department, Government of Bihar was approached. The required input parameters such as soil unit weight, shear strength parameters, saturated hydraulic conductivity etc. have been obtained from the Design report of Durgawati reservoir project [34].

Results and Discussion

Seepage Analysis

Figure 2 shows the result of seepage analysis for the two dam sections i.e. at sections CH 21.00 and CH 22.00 respectively. In these two figures, the initial (i.e. at 0 days) and final water level after 57 days have been shown. The topmost flow line inside the embankment slope reflects the phreatic for steady state seepage condition. The bottommost flow line reflects the phreatic surface after carrying out transient seepage analysis. As the saturated conductivity is 100 times less in the core material than the shell material, a considerable drop in the total head of the water is evident from the results. It is observed that a good portion of the reservoir total head is lost in the core of the embankment.

Since, the water level in the reservoir is changed gradually with time from "Initial water level" (H = 128. 6 m) to a "dead storage level" (H = 109.4 m) during the period of first 10 days, the resulting water flow lines in the saturated zone (i.e. phreatic surface) are also changing inside the embankment. In addition, it also evident from Fig. 2, that the dissipation of water inside the embankment is not as quick as in the reservoir due to the much lower conductivity of embankment materials. Because of this reason, water inside the embankment takes 57 days or more to dissipate completely. Figure 2 also shows how the phreatic surface is gradually changing with respect to time during the drawdown process. However, water in the reservoir comes down to the dead storage level after 10 days of the beginning of the drawdown process.

Stability Analysis

In this section, the results and corresponding plots of stability analyses of Durgawati earthen embankment have been presented. Only the relevant plots obtained using Bishop's method [4, 5] have been presented in Figs. 3, 4, 5, 6, 7, 8, 9, 10, 11, 12, 13, 14 and 15 for downstream slopes and in Figs. 13, 14, 15, 16, 17, 18, 19, 20, 21, 22, 23, 24, 25, 26, 27 and 28 for upstream slopes. Because the nature of relevant plots obtained from Morgenstern and Price [8] and Corps of Engineers [12] are similar to that of Bishop's method [4, 5], they have not been shown in this paper. Only the values of FOS obtained from Morgenstern and Price [8] and Corps of Engineers [12] have been presented in Tables 2 and 5. Also, it is observed that the Bishop's method yields the most conservative results from these two tables.

Factor of Safety (FOS) of Downstream Slope Section at CH 21.00 and CH 22.00

Table 2 presents the FOS values against slope failure for static and seismic slope stability analysis of downstream slope section at CH 21.00 and CH 22.00 for different cases as described in "Model Analysis".

Effect of Drawdown on Static FOS

Figure 3 shows the FOS value and associated critical failure surface for the static slope stability analysis for Case-1 at CH 21.00 and CH 22.00 respectively. In addition,

Table 1 Properties of different component of Durgawati Earthen Embankment Dam

Soil designation	Effective cohesion C (kPa)	Friction angle φ (degree)	Unit weight γ (KN/m^3)	Saturated conductivity k (m/s)
Embankment core	20.0	24.5	21.07	1×10^{-7}
Embankment shell	15.0	24.5	21.07	1×10^{-5}
Foundation	10.0	30	20.08	1×10^{-5}
Filter	0.0	24.5	16.50	1×10^{-4}
Toe drain	0.0	24.5	16.50	0.5

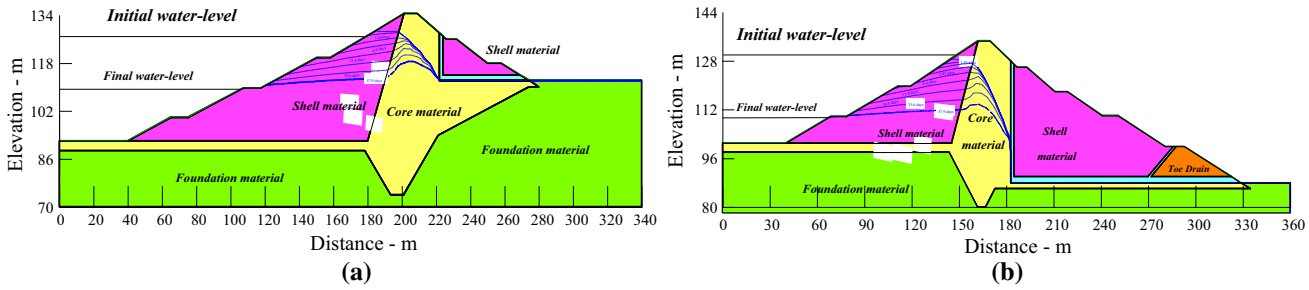

Fig. 2 Different zero pressure phreatic line during transient-seepage analysis for sections: **a** CH 21.00 and **b** CH 22.00

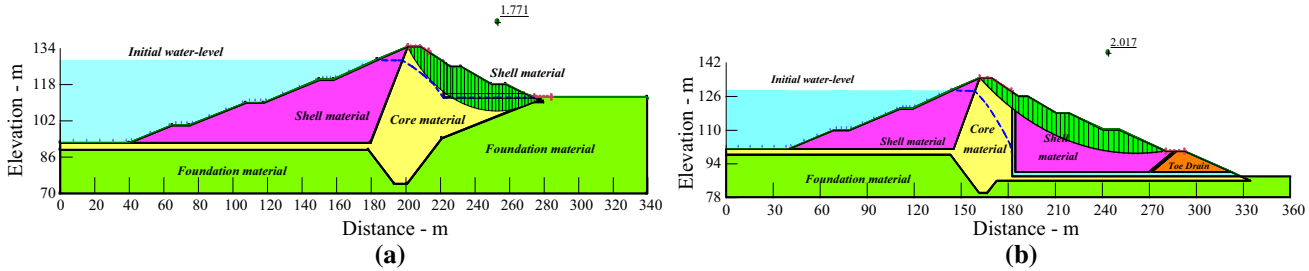

Fig. 3 Failure surface and corresponding FOS value for Case-1 at sections: **a** CH 21.00 and **b** CH 22.00

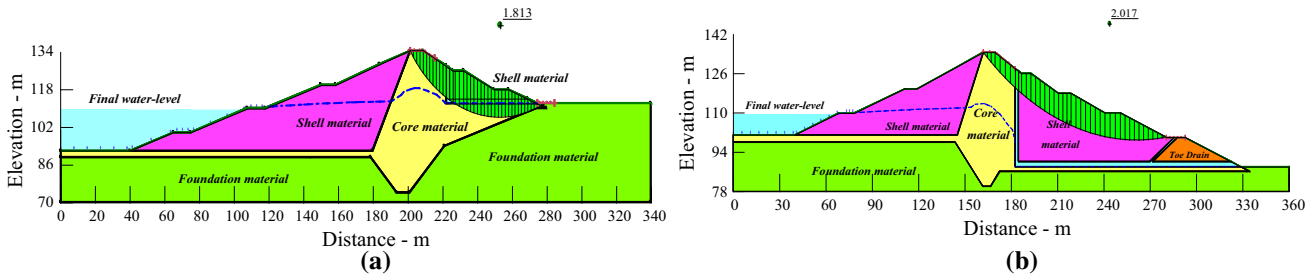

Fig. 4 Failure surface and corresponding FOS value for Case-2 at sections: **a** CH 21.00 and **b** CH 22.00

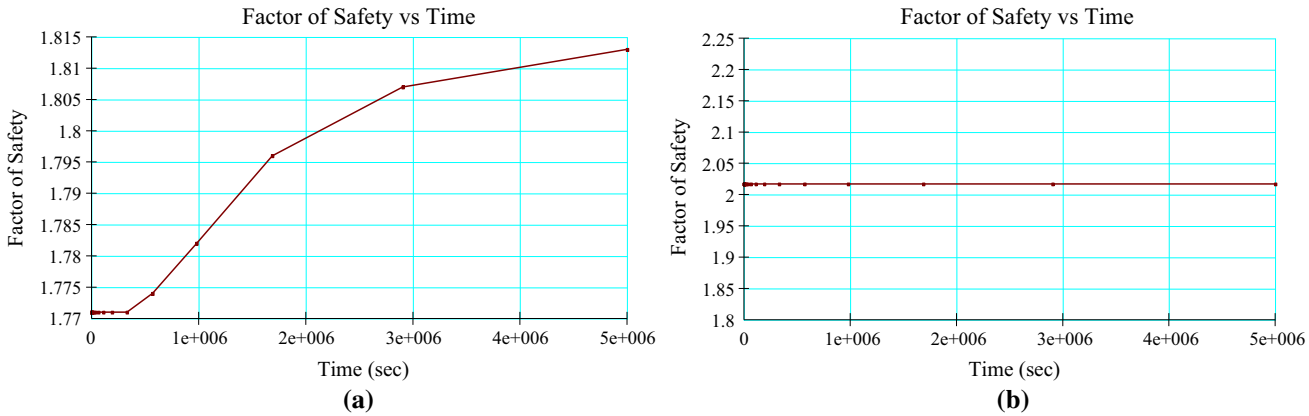

Fig. 5 Effect of drawdown on FOS value at sections: **a** CH 21.00 and **b** CH 22.00

Fig. 4 shows the FOS value and associated critical failure surface for the static slope stability analysis for Case-2.

For Case-1, minimum Static FOS value against slope failure for downstream slope stability analysis at CH 21.00 is found out to be equal to 1.77 whereas, minimum FOS value at CH 22.00 is 2.017. For Case-2, FOS value at CH 21.00 has increased marginally by 0.62% and found out to be 1.782 just after 10 days of drawdown (i.e. when water-

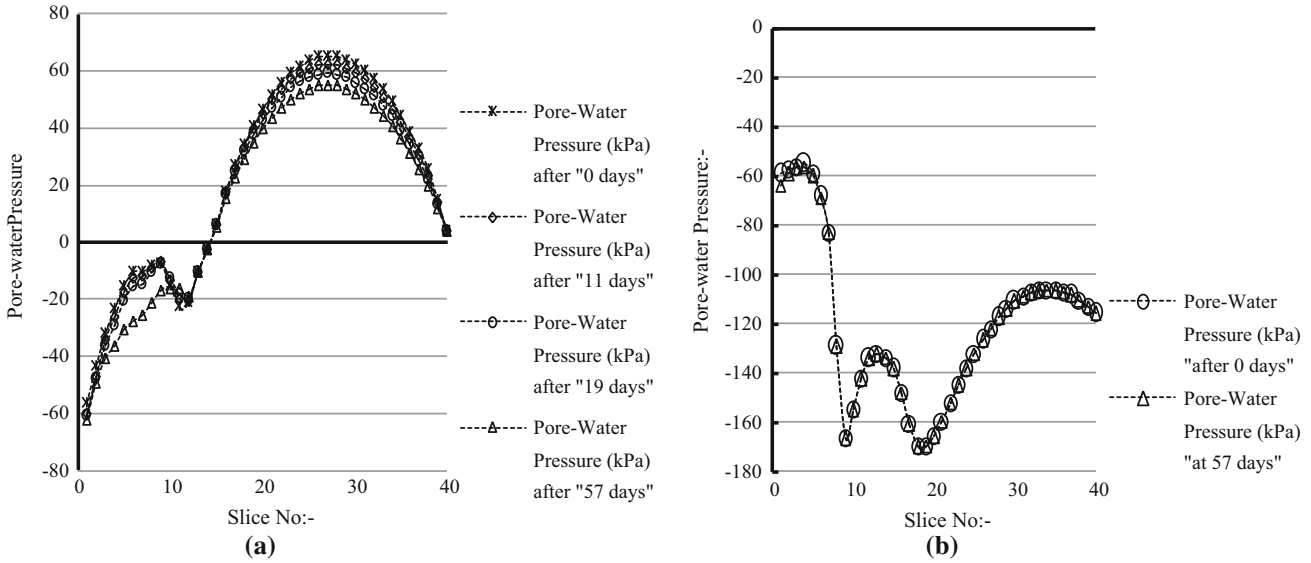

Fig. 6 Development of pore-pressure during transient-state seepage at sections: **a** CH 21.00 and **b** CH 22.00

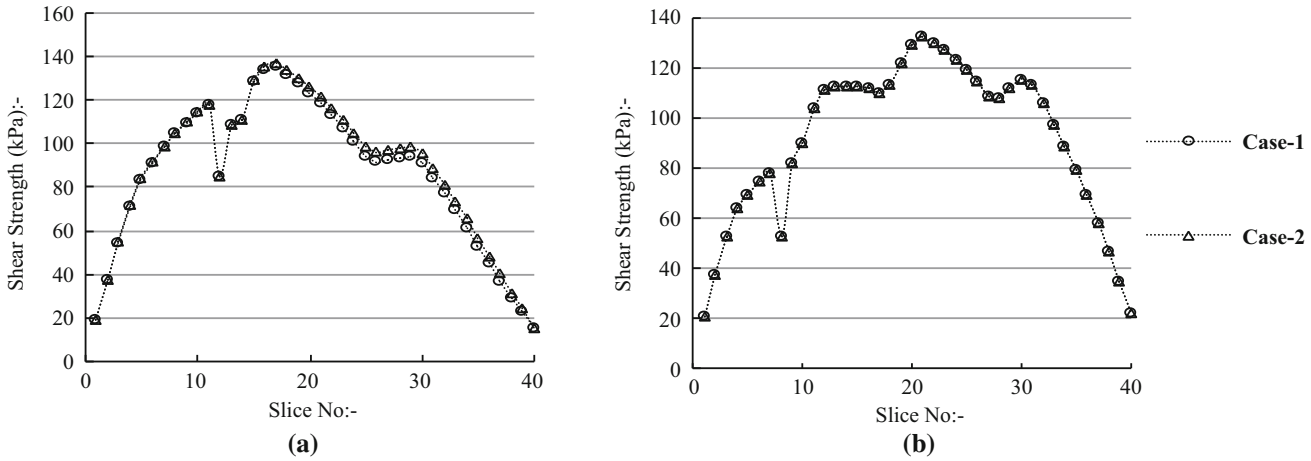

Fig. 7 Comparison of shear strength for Case-1 and Case-2 at sections: **a** CH 21.00 and **b** CH 22.00

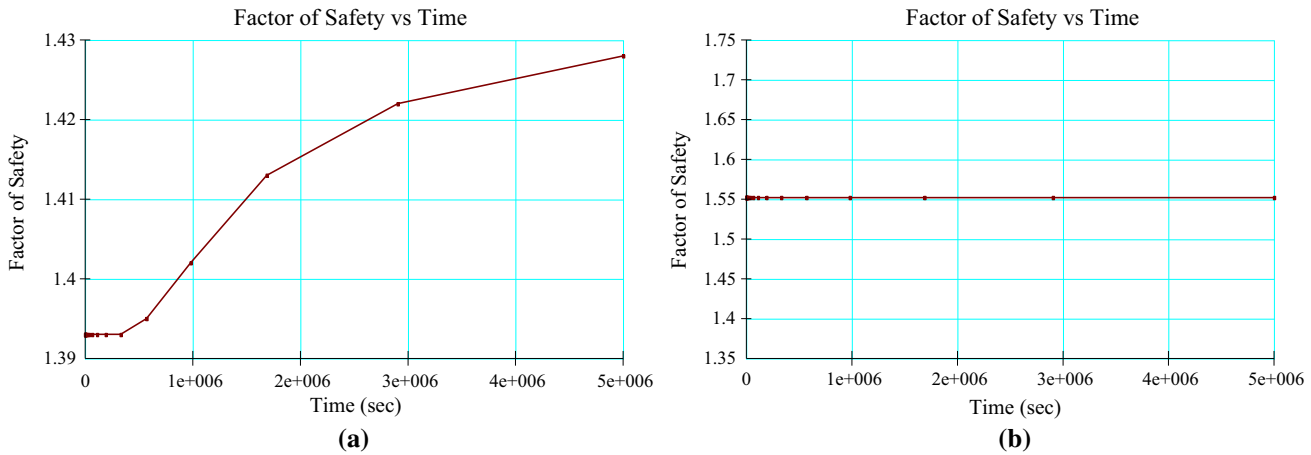

Fig. 8 Effect of drawdown on FOS value at sections: **a** CH 21.00 and **b** CH 22.00

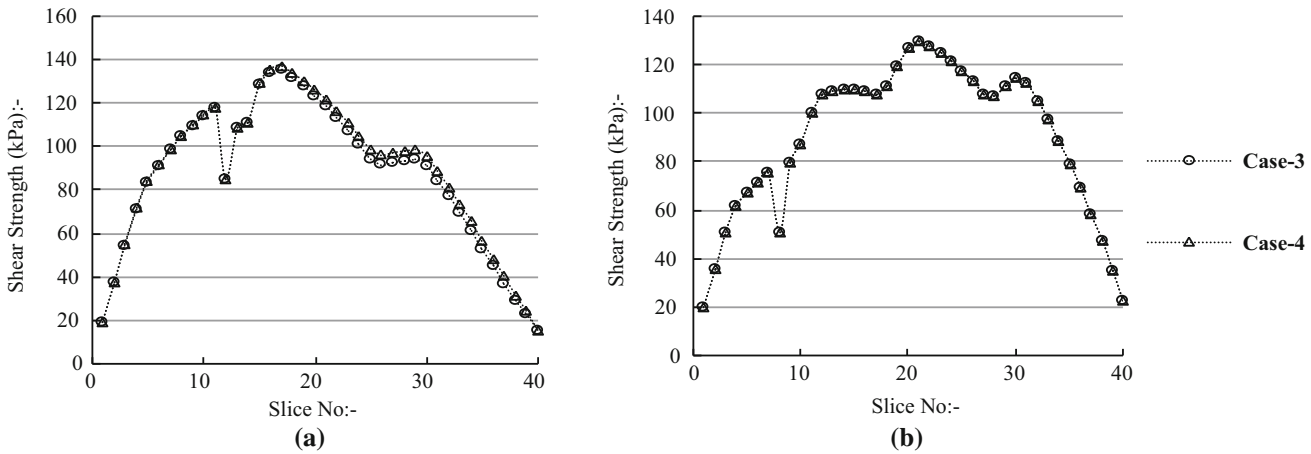

Fig. 9 Comparison of shear strength for Case-3 and Case-4 at sections: **a** CH 21.00 and **b** CH 22.00

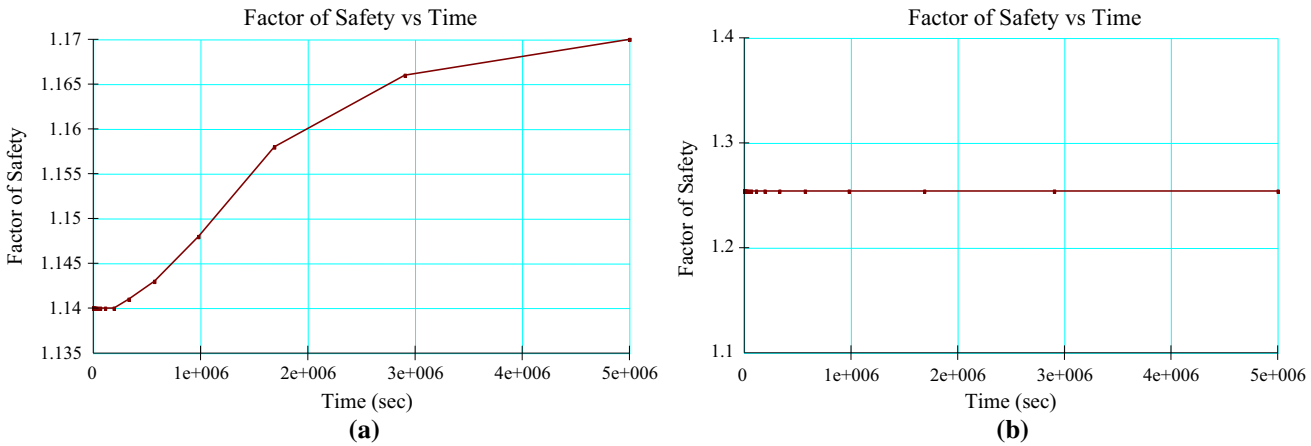

Fig. 10 Effect of drawdown on FOS value at sections: **a** CH 21.00 and **b** CH 22.00

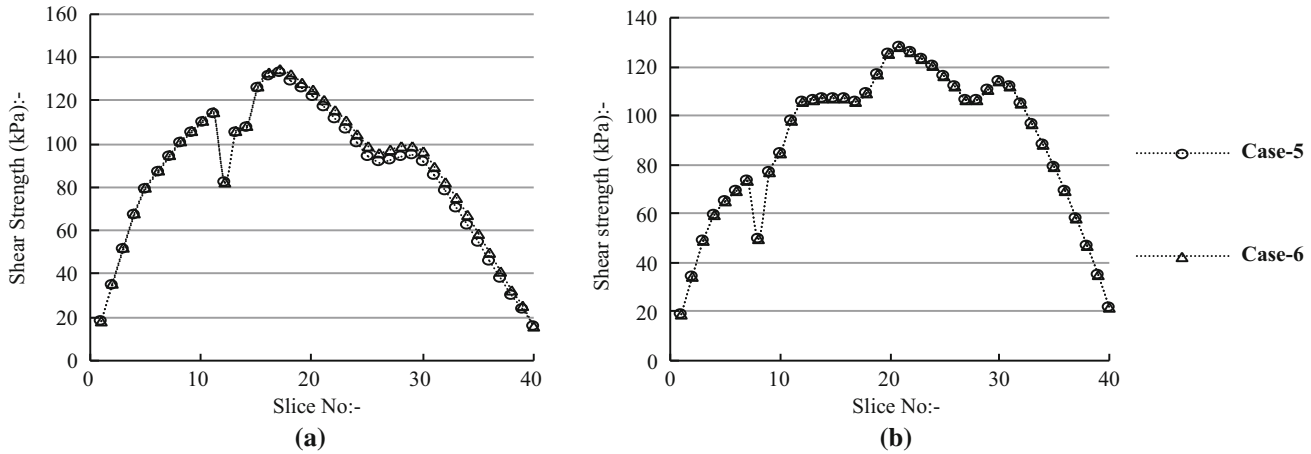

Fig. 11 Comparison of shear strength for Case-5 and Case-6 at sections: **a** CH 21.00 and **b** CH 22.00

level in the reservoir has reached the dead storage level). From Fig. 5a, it is observed that the FOS value increases with time by 2.4% and is found to be 1.813 after 57 days as the excess pore water pressure dissipates. FOS value against slope failure remains constant with time during the drawdown process for slope at CH 22.00. This is because the phreatic surface does not pass through the failure surface during Case-1 and Case-2 as evident from Figs. 3b

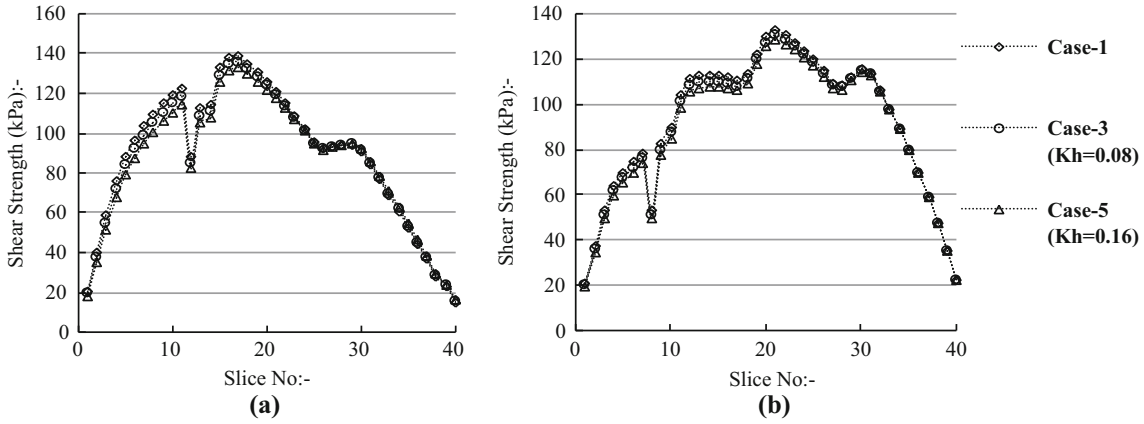

Fig. 12 Comparison of shear strength for Case-1, Case-3 and Case-5 at sections: **a** CH 21.00 and **b** CH 22.00

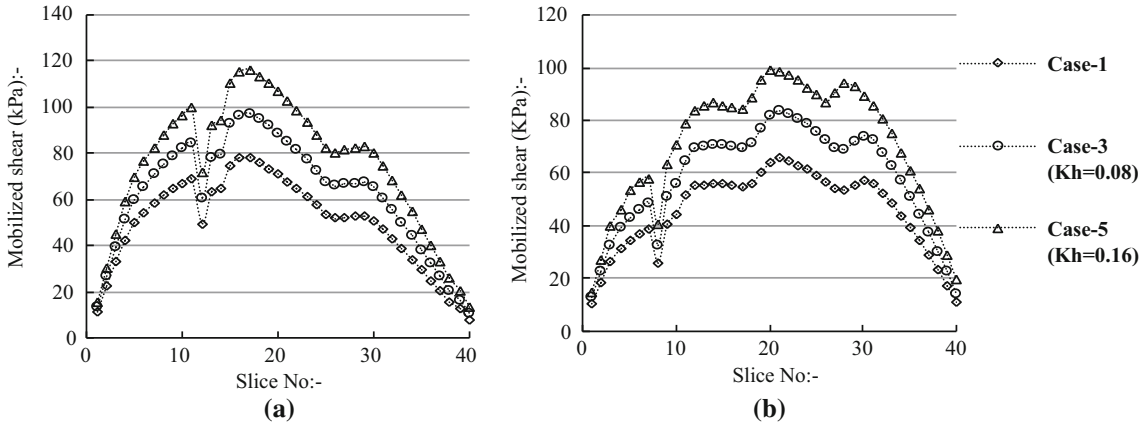

Fig. 13 Comparison of mobilized shear for Case-1, Case-3 and Case-5 at sections: **a** CH 21.00 and **b** CH 22.00

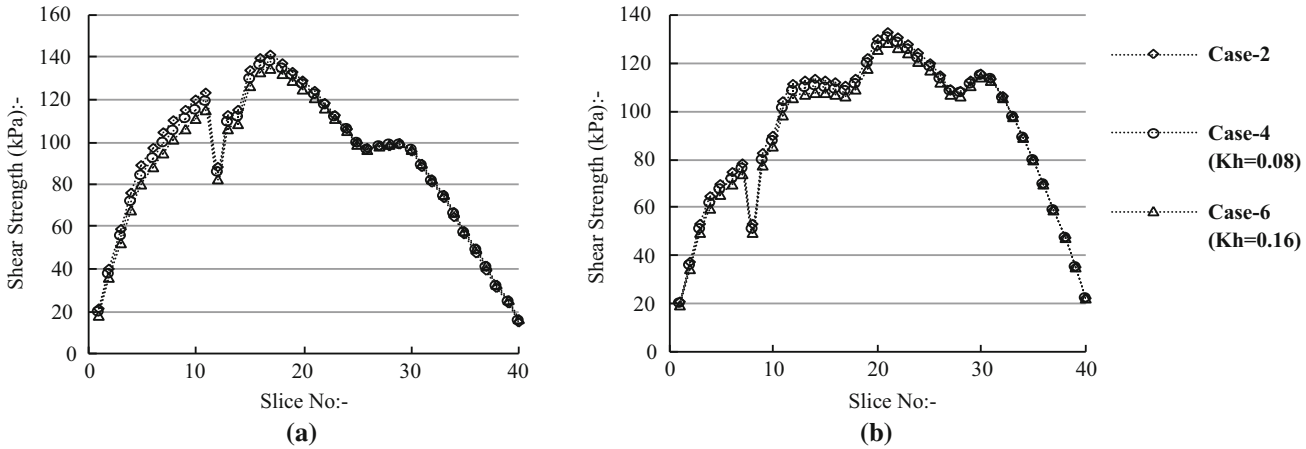

Fig. 14 Comparison of shear strength for Case-2, Case-4 and Case-6 at sections: **a** CH 21.00 and **b** CH 22.00

and 4b. Therefore, the resulting pore water pressure does not affect the slope analyses in both the cases. In addition, as the drawdown in the reservoir begins the reduction of water from the reservoir and dissipation of pore water from embankment material is a function of time during the entire process of drawdown. Consequently, the FOS value linked with the slope also become function of time. Figure 4 shows the variation in the FOS with time during and after drawdown of 10 days for the two slope sections at CH 21.00 and CH 22.00, respectively.

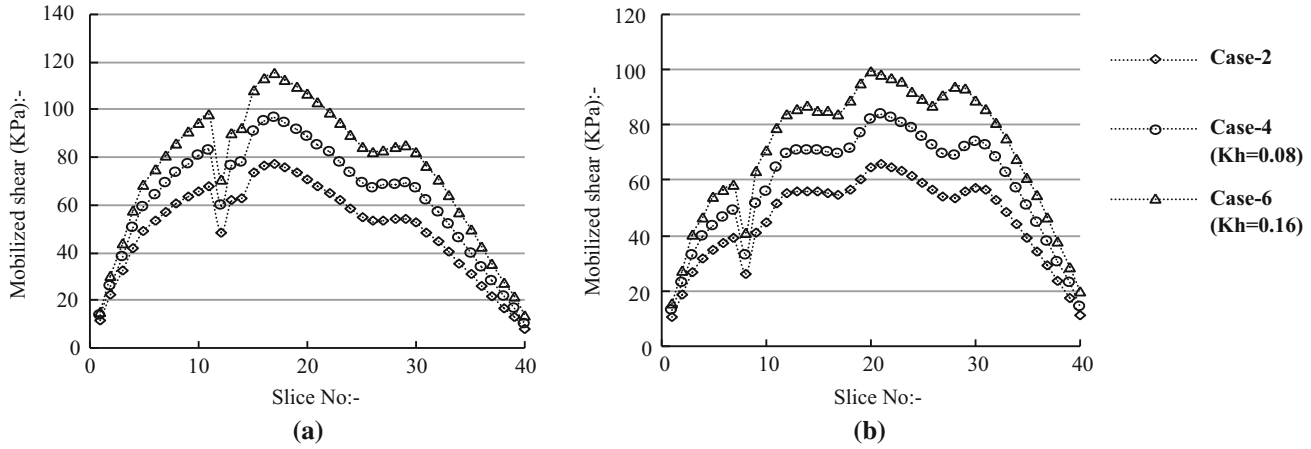

Fig. 15 Comparison of mobilized shear for Case-2, Case-4 and Case-6 at sections: **a** CH 21.00 and **b** CH 22.00

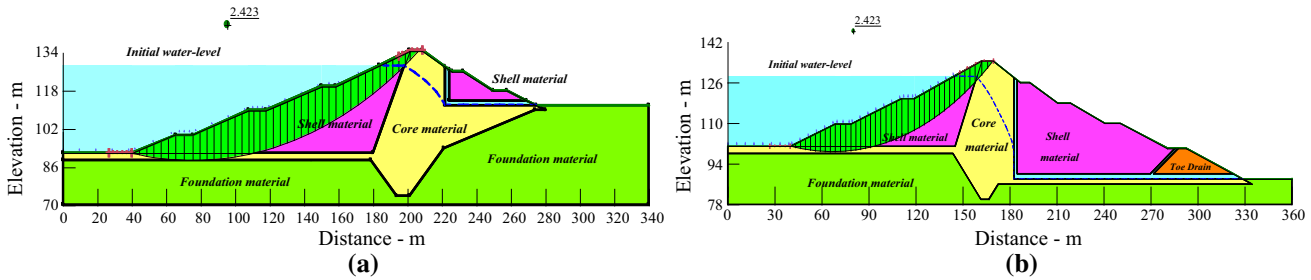

Fig. 16 Failure surface and corresponding FOS value for Case-1 at sections: **a** CH 21.00 and **b** CH 22.00

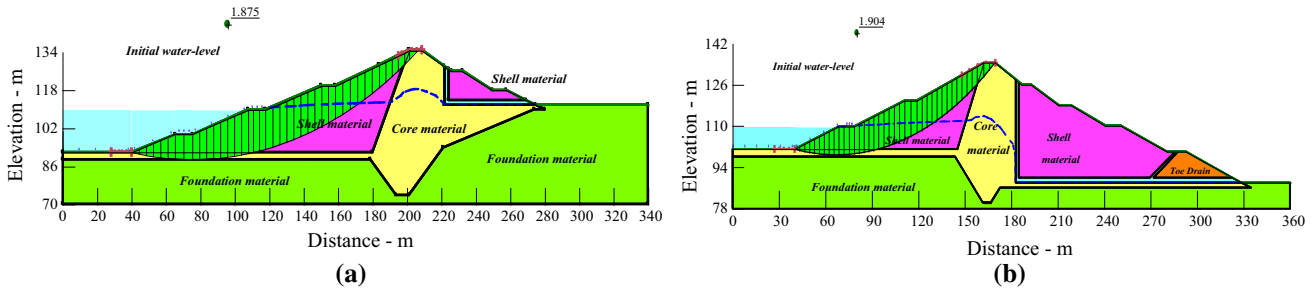

Fig. 17 Failure surface and corresponding FOS value for Case-2 at sections: **a** CH 21.00 and **b** CH 22.00

It is observed from Fig. 5a that the variation of FOS value up to 4 days is very less. As the process of drawdown starts, the head difference between the reservoir water level and that inside the embankment slowly begins to increase with time. Initially, this difference is very less during first 4 days resulting into very little change in phreatic surface as shown in Fig. 2a. Figure 6a shows the variation of pore water pressure values at the beginning of drawdown process, after 11 days and after 57 days respectively along the slices associated with failure slip surface for CH 21.00. It also reflects much less dissipation of pore water pressure during the period of first 4 days. That is why; the FOS value remains nearly constant during this time. Furthermore, the water level in the res7ervoir continuously reduces to dead storage level at the end of 10th day and the drawdown process ends. At that point of time, the head difference is maximum. But, the resulting phreatic surface reduces at a slower rate inside the embankment because the permeability of the embankment material is relatively less. Figure 2a depicts the lowering of phreatic surfaces at different times after the drawdown process has begun. The corresponding dissipation of excess pore water pressure with time is shown in Fig. 6a. The pore water pressure along each individual slices are shown in Fig. 6a for the slope section at CH 21.00 at 0 days, 11 and 57 days, respectively. After 4 days, the FOS value begins to increase slowly up to 57th day as the dissipation of excess pore-pressure takes place. Corresponding increase in shear strength along the failure surface is depicted in Fig. 7a.

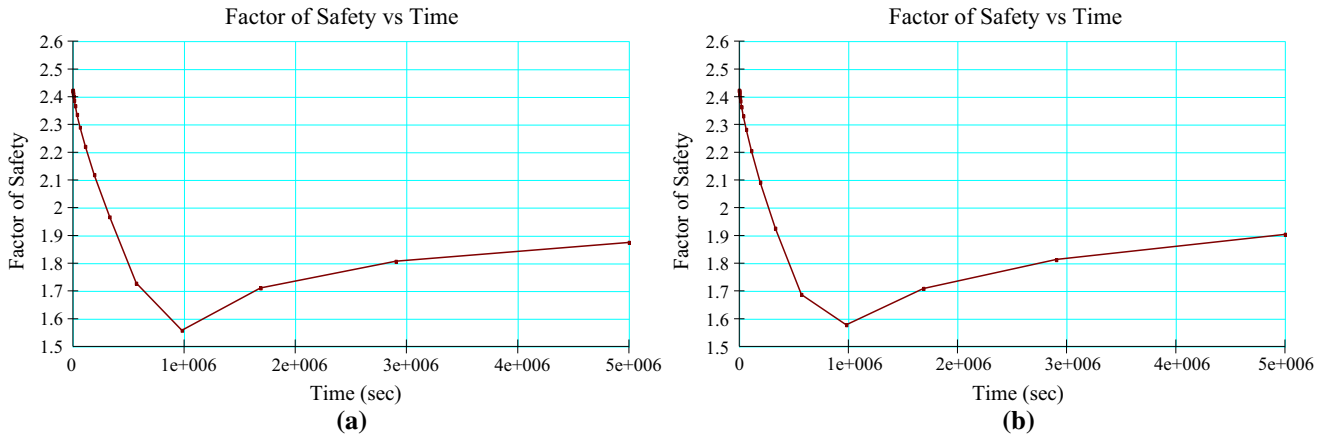

Fig. 18 Effect of drawdown on FOS value at sections: **a** CH 21.00 and **b** CH 22.00

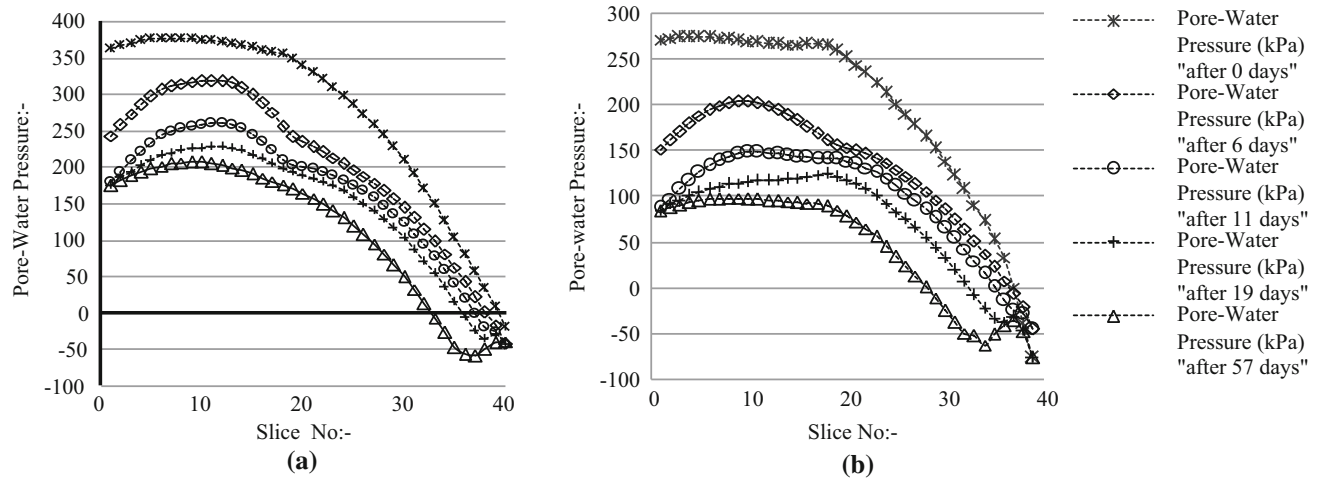

Fig. 19 Different pore-pressure during transient-state seepage at sections: **a** CH 21.00 and **b** CH 22.00

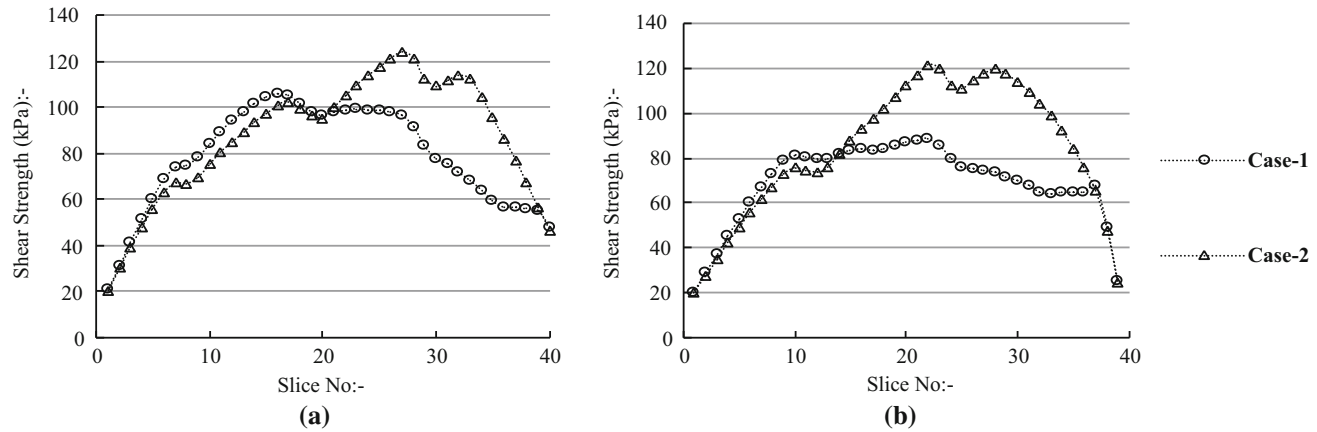

Fig. 20 Comparison of shear strength for Case-1 and Case-2 at sections: **a** CH 21.00 and **b** CH 22.00

Whereas, Fig. 5b, shows that FOS value remain constant with time during and after 10 days of drawdown for slope at CH 22.00. This FOS value remains constant because the phreatic surface does not pass through the potential failure surface of the slope at CH 22.00 for both Case-1 and Case-2 as shown in Figs. 3b and 4b. The negative pore water pressure is generated when the failure slip surface is above the phreatic line and the positive

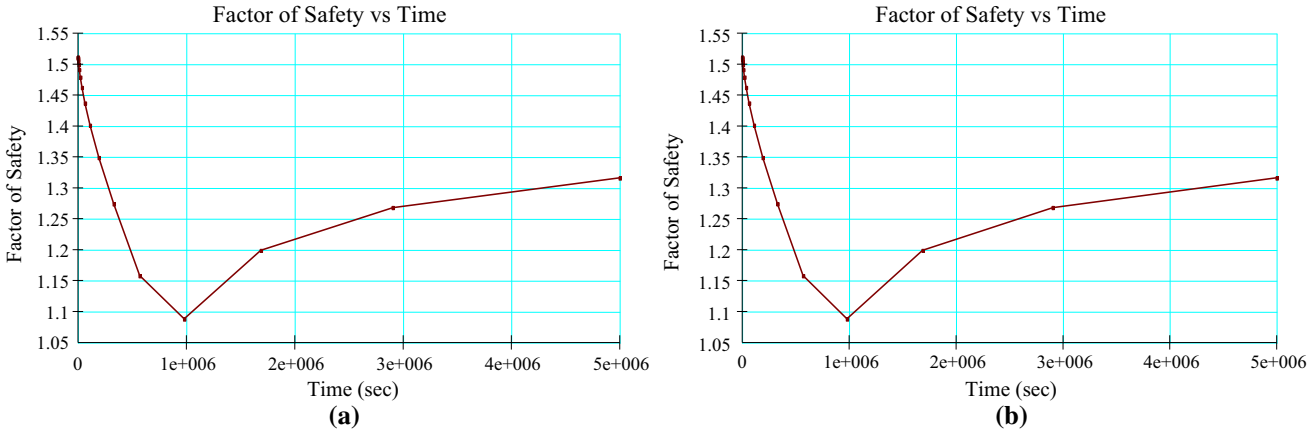

Fig. 21 Effect of drawdown on FOS value at sections: **a** CH 21.00 and **b** CH 22.00

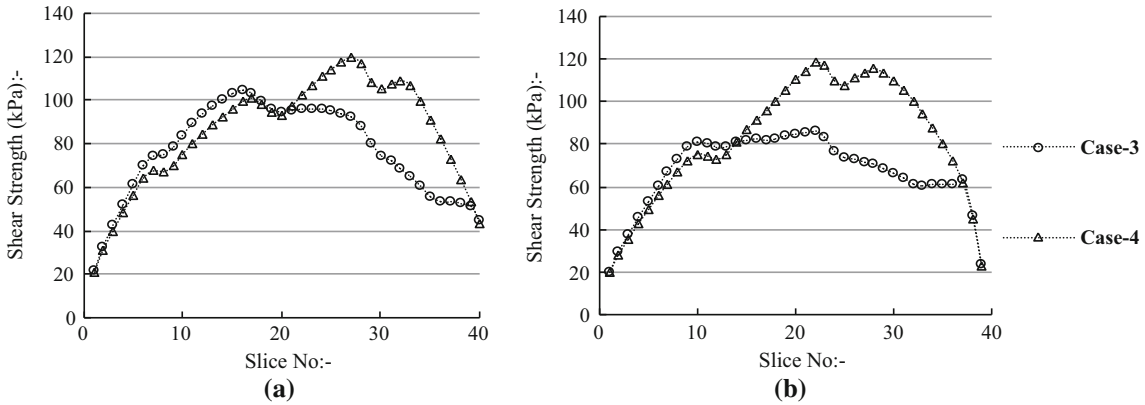

Fig. 22 Comparison of shear strength for Case-3 and Case-4 at sections: **a** CH 21.00 and **b** CH 22.00

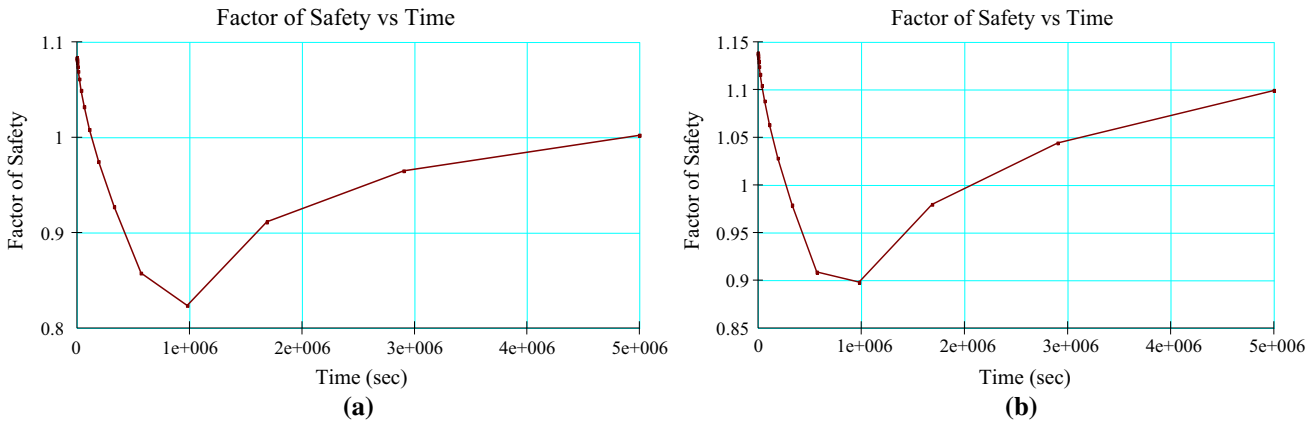

Fig. 23 Effect of drawdown on FOS value at sections: **a** CH 21.00 and **b** CH 22.00

pore water pressure develops when the phreatic surface passes through the failure slip surface. For CH 22.00, the pore water pressure developed along the each individual slice of slip surface is negative as shown in Fig. 6b. This indicates that the phreatic surface never intersects the failure slip surface during the period of 57 days. Therefore, the shear strength of the slices associated with the failure mass will remain constant and this phenomenon is represented in Fig. 7b.

In Fig. 7 sudden drop of shear strength is observed for the slopes i.e. at CH 21.00 and CH 22.00, respectively. It is because the failure surface is passing through the chimney drain where the shear strength properties are considerably less than that of core and the shell material.

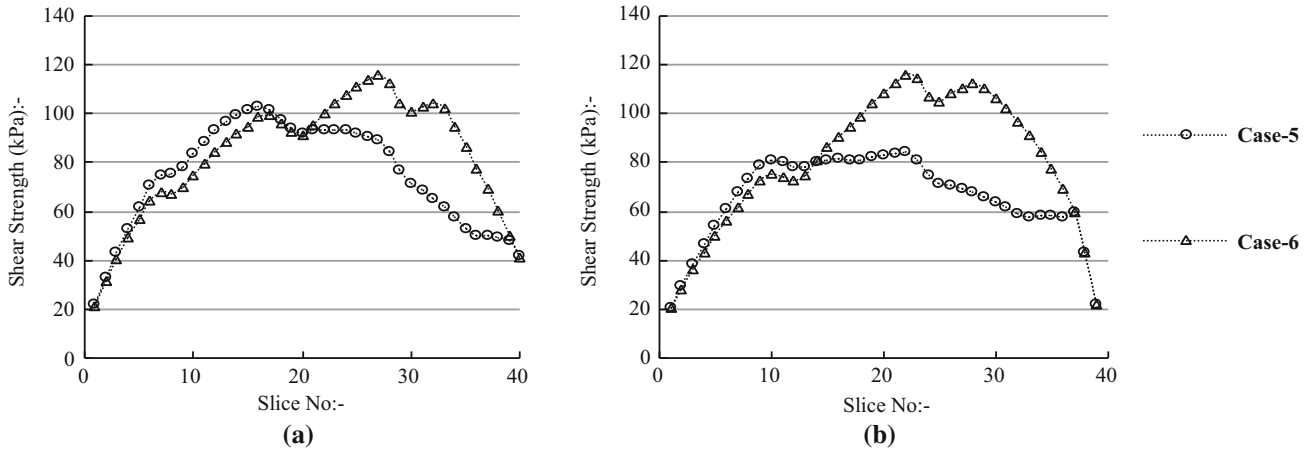

Fig. 24 Comparison of shear strength for Case-5 and Case-6 at sections: **a** CH 21.00 and **b** CH 22.00

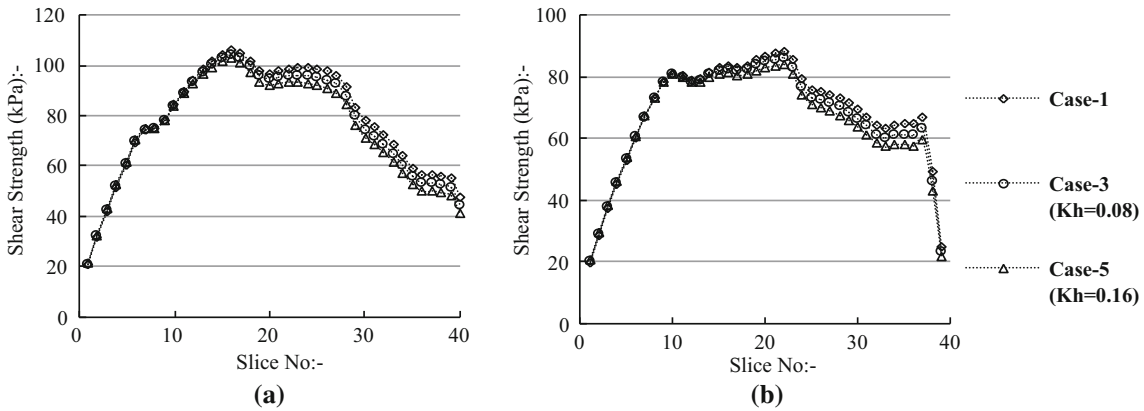

Fig. 25 Comparison of shear strength for Case-2, Case-4 and Case-6 at sections: **a** CH 21.00 and **b** CH 22.00

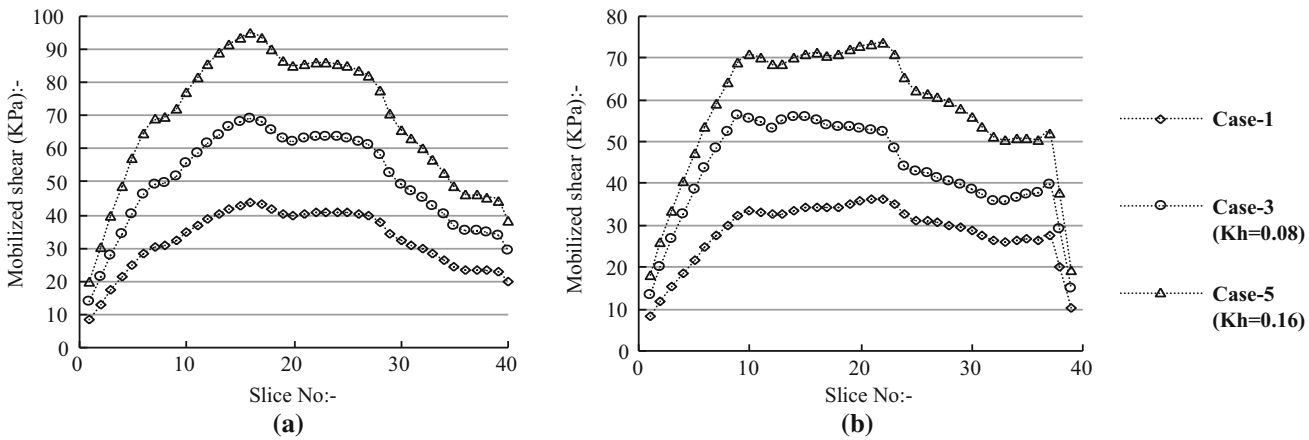

Fig. 26 Comparison of mobilized shear for Case-2, Case-4, and Case-6 at sections: **a** CH 21.00 and **b** CH 22.00

Effect of Drawdown on Seismic FOS

For Horizontal Seismic Coefficient $k_h = 0.08$

Seepage and stability analyses are carried out for the slopes at CH 21.00 and CH 22.00 respectively when seismic horizontal force of magnitude ($k_h = 0.08$) is applied. From Table 2, it is observed that for Case-3, FOS value against slope failure for downstream slope stability analysis at CH 21.00 is 1.393 whereas the same is equal to 1.552 for CH 22.00. For Case-4, FOS value at CH 21.00 improves slightly by 0.64% and found to be 1.402 just after 10 days

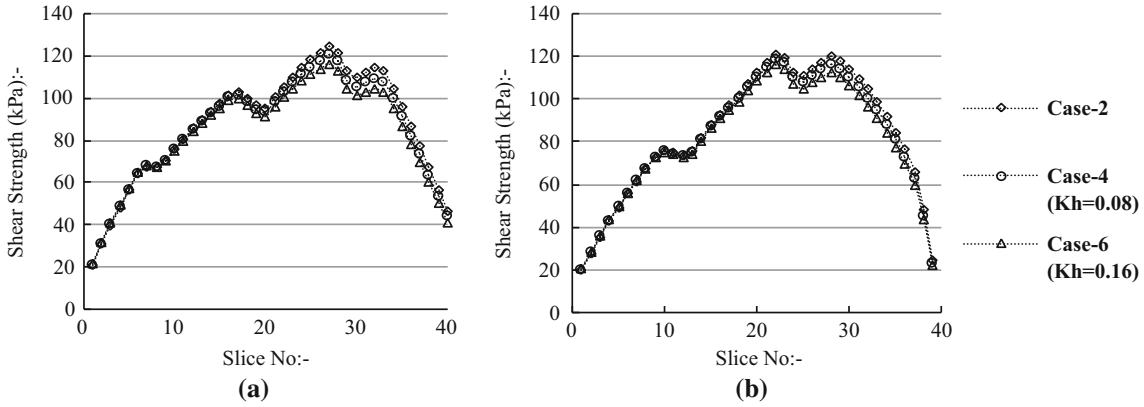

Fig. 27 Comparison of shear strength for Case-2, Case-4 and Case-6 at sections: **a** CH 21.00 and **b** CH 22.00

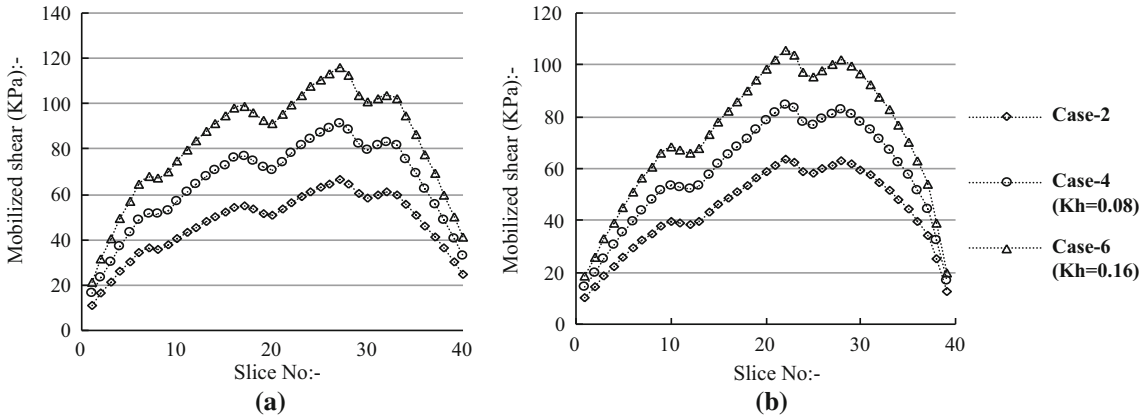

Fig. 28 Comparison of Shear Strength for Case-2, Case-4 and Case-6: **a** CH 21.00 and **b** CH 22.00

Table 2 Factor of safety (FOS) for downstream slope section at CH 21.00 and CH 22.00

Reservoir conditions	Factor of safety Bishop's method (1950)		Factor of safety Morgenstern and Price (1965)		Factor of safety Corps of Engineers (1970)	
	CH 21.00	CH 22.00	CH 21.00	CH 22.00	CH 21.00	CH 22.00
Case-1	1.771	2.017	1.770	2.016	1.788	2.020
Case-2	1.813	2.017	1.813	2.016	1.832	2.020
Case-3 ($k_h = 0.08$)	1.393	1.552	1.397	1.553	1.509	1.712
Case-4 ($k_h = 0.08$)	1.428	1.552	1.431	1.553	1.541	1.712
Case-5 ($k_h = 0.16$)	1.140	1.254	1.149	1.225	1.216	1.437
Case-6 ($k_h = 0.16$)	1.170	1.254	1.178	1.255	1.249	1.437

of drawdown (i.e. water level in the reservoir is at dead storage level). The FOS value is observed to increase with time by 2.6% as the excess pore-pressure dissipates as shown in Fig. 8a. In these two cases, the variation of pore pressures along failure slip surface will be same as that in case of Case-1 and Case-2 respectively because all conditions related to seepage analyses are exactly similar. After 57 days, the FOS value increases to 1.428. The FOS value against slope failure remains constant with time during the drawdown process for slope at CH 22.00. Figure 8 shows the variation in the FOS with time during and after drawdown of 10 days for the two slope sections at CH 21.00 and CH 22.00 respectively.

Moreover, Fig. 8a, also exhibits that the FOS value is nearly constant up to 4 days and then increases for slope at CH 21.00 for Case-3. Whereas, Fig. 8b shows that FOS for

value remain constant with time during and after 10 days of drawdown for slope at CH 22.00. For the results shown in Case-3 and Case-4 (i.e. Figs. 8, 9), the explanations can be given similarly as for Case-1 and Case-2 respectively.

Effect of Drawdown on Seismic FOS

For Horizontal Seismic Coefficient $k_h = 0.16$

For Case-5, minimum FOS value against slope failure for downstream slope stability analysis at CH 21.00 is found out to be equal to 1.140 whereas, the FOS value at CH 22.00 is 1.254. For Case-6, FOS value at CH 21.00 increases by 0.70% to 1.148 just after 10 days of drawdown (i.e. when water-level in the reservoir is at dead storage level). The FOS value increases with time by 1.9% to 1.170 after 57 days as the excess pore-pressure dissipates as shown in Fig. 13a. The results of seepage analyses of case 5 and case 6 will be same as that of Case-1 and Case-2 respectively because the seepage conditions are similar. The FOS value against slope failure remains constant with time during the entire drawdown process for slope at CH 22.00. Figure 13 shows the variation in the FOS with time during and after drawdown of 10 days for the two slope sections at CH 21.00 and CH 22.00 respectively.

Moreover, Fig. 10a also shows that the FOS for value is nearly constant up to 2 days and then increases for slope at CH 21.00. Whereas, Fig. 10b shows that FOS for value remain constant with time during and after 10 days of drawdown for slope at CH 22.00. Similar conclusions like Case-1 and Case-2, regarding the improvement of the FOS against slope failure for slope at CH 21.00 and constant FOS for slope at CH 22.00 remain applicable for this case. A comparison of shear strength for Case-5 and Case-6 for slope at section CH 21.00 and CH 22.00 are presented in Fig. 11.

Effect of Seismic Acceleration on Static FOS, Shear Strength and Mobilized Shear

For Constant reservoir water-level (i.e. Steady-State Seepage)

Table 3 presents the FOS values against failure of downstream slope for Case-1, Case-3 and Case-5 at CH 21.00 and CH 22.00, respectively. The percentage increase and decrease of FOS values with respect to that of Case-1 is also presented.

Figure 12 shows the effect of horizontal acceleration on shear strength profile for slope section at CH 21.00 and CH 22.00 respectively. The comparisons are made for Case-1, Case-3 and Case-5 respectively. In all these three cases, the seepage conditions are same (i.e. steady-state seepage condition). From Eq. (10), it is observed that the application of horizontal seismic loading decreases the magnitude of shear strength along failure surface by an amount $(k_h W Sin\alpha)$ from that of the static analysis (Eq. 6). However, the application of seismic load has large influence on mobilized shear and magnitude of mobilized shear increases by $(k_h W Cos\alpha)$ as shown by Eq. (11) compared to the static analysis (Case-1) where the mobilized shear along individual slice is expressed in Eq. (7). Figure 13 shows the effect of horizontal acceleration on mobilized shear profile for slope section at CH 21.00 and CH 22.00, respectively. It is observed that the mobilized shear is maximum for seismic analysis when $k_h = 0.16$ in comparison to the static case as expected.

Effect of Seismic Acceleration on Static FOS, Shear Strength and Mobilized Shear

For Drawdown in Reservoir Water Level (i.e. Transient-State Seepage)

Table 4 presents the FOS values against failure of downstream slope for Case-2, Case-4 and Case-6 at CH 21.00 and CH 22.00, respectively. The percentage decrease of FOS values with respect to that of Case-2 is also presented.

The comparisons are made for Case-2, Case-4 and Case-6 respectively. In all these three cases, the transient seepage state is considered to simulate the drawdown phenomenon in the reservoir. Figure 14 shows the effect of applied horizontal seismic acceleration on shear strength profile for slope section at CH 21.00 and CH 22.00 respectively. Whereas, Fig. 15 shows the effect of horizontal acceleration on mobilized shear for slope section at CH 21.00 and CH 22.00 respectively. Similar conclusions like comparison of Case-1, Case-3 and, Case-5 regarding the effect of seismic load on shear strength and mobilized shear respectively are applicable here.

From Tables 3 and 4, it may be observed that the percentage decrease in FOS values is almost same. These two tables reflect the effect of earthquake under the application of different horizontal seismic coefficient (k_h) independently. Table 3 shows the percentage decrease in FOS value for the respective cases having similar seepage condition with full reservoir level whereas Table 4 is for situation after 57 days. Referring to Eqs. (10) and (11), it can be seen that the shear strength and mobilized shear and the corresponding FOS against slope failure are dependent on the weight of the failure mass, which is the summation of weight W of individual slices as well as the horizontal seismic coefficient (k_h).

It is observed from Figs. 3b and 4b that the phreatic line never intersects the failure surface for CH 22.00. Therefore, the effective weight each individual slice W as well as that of the failure mass considered in the slope analysis remains unchanged. That is why; the calculated FOS values of downstream slope for CH 22.00 do not change as shown in Tables 3 and 4. From Figs. 3a and 4a, it can be observed that the phreatic surface passes through the failure mass but

Table 3 Percentage change in factor of safety (FOS) for downstream slope

Embankment Dam conditions	FOS at CH 21.00	% Decrease in FOS	FOS at CH 22.00	% Decrease in FOS
Case-1	1.771	21.3%	2.017	23.1%
Case-3 ($k_h = 0.08$)	1.393		1.552	
Case-1	1.771	35.6%	2.017	37.8%
Case-5 ($k_h = 0.16$)	1.140		1.254	

Table 4 Percentage change in factor of safety (FOS) for downstream slope

Embankment Dam conditions	FOS at CH 21.00	% Decrease in FOS	FOS at CH 22.00	% Decrease in FOS
Case-2	1.813	21.2%	2.017	23.1%
Case-4 ($k_h = 0.08$)	1.428		1.552	
Case-2	1.813	35.5%	2.017	37.8%
Case-6 ($k_h = 0.16$)	1.170		1.254	

it is primarily arrested in the drainage path inside the dam body. This is true for the analysis for full reservoir condition as well as for the analysis after 57 days. Comparing Figs. 3a and 4a, it can be seen that change in the portion of submerged failure mass is very less in both scenarios. That is why, with each increment of horizontal seismic coefficient, the percentage change in estimated FOS values for Case-1, Case-3 and Case-5 and for Case-2, Case-4 and Case-6 are almost similar.

Factor of Safety (FOS) of Upstream Slope Section at CH 21.00 and CH 22.00

Table 5 presents the FOS values against slope failure for static and seismic slope stability analysis of upstream slope section at CH 21.00 and CH 22.00 for different cases as described in "Model Analysis".

Effect of Drawdown on Static FOS

Figure 16 shows the FOS value and associated critical failure surfaces for the static slope stability analyses for Case-1 at CH 21.00 and CH 22.00 respectively. In addition, Fig. 17 shows the FOS value and associated critical failure surfaces for the static slope stability analyses for Case-2 at CH 21.00 and CH 22.00 respectively.

For Case-1, minimum static FOS value against slope failure for upstream slope stability analysis at CH 21.00 is observed as 2.423 whereas the FOS value at CH 22.00 is found out to be equal to 2.423. For Case-2, FOS value at CH 21.00 decreases significantly by 35.7% to 1.558 just after 10 days of drawdown (i.e. water level in the reservoir is at dead storage level). However, it is observed that the FOS value recovers with time by 13.1% as the excess pore-pressure dissipates and becomes 1.875 after 57 days. A similar behavior in FOS value during the drawdown process is observed for slope at CH 22.00 with initial decrease in FOS value by 34.9% to 1.578 after 10 days of drawdown and finally the FOS value recovers by 13.5% and found to be 1.904 after 57 days.

It is evident from Fig. 18 that the FOS value decreases initially during the period of 10 days for the two slope sections at CH 21.00 and CH 22.00 respectively. As the process of drawdown starts, the water level in the reservoir continuously reduces to dead storage level at the end of 10th day and the drawdown process ends. However, the resulting phreatic surface lowers at a slower rate inside the embankment because the permeability of the embankment material is relatively less. The presence of water inside the reservoir act as a stabilizing force for the upstream slope. The reduction of FOS value during initial 10 days is due to sudden decrease of stabilizing force resulting from lowering of reservoir water level in the upstream side of the embankment. There is no further reduction in the water level after 10 days and the excess pore pressure gradually dissipates inside the embankment up to 57th days. This leads to slow but gradual appreciation of FOS value of the slope against failure process and after 6, 11, 19 and 57 days respectively along the slices associated with failure slip surface for CH 21.00 and CH 22.00. However, after initial decrease in FOS value during the period of 10 days, the FOS value gradually improves up to 57th day as dissipation of excess pore-pressure takes place inside the embankment (as explained before) as shown in Fig. 19 for both the slope at CH 21.00 and CH 22.00 respectively. This also improves the shear strength associated with each individual slice as shown in Fig. 20. This phenomenon, in turn improves

Table 5 Factor of safety (FOS) for upstream slope section at CH 21.00 and CH 22.00

Reservoir conditions	Factor of safety Bishop's method (1950)		Factor of safety Morgenstern and Price (1965)		Factor of safety Corps of Engineers (1970)	
	CH 21.00	CH 22.00	CH 21.00	CH 22.00	CH 21.00	CH 22.00
Case-1	2.423	2.423	2.423	2.422	2.717	2.662
Case-2	1.875	1.904	1.875	1.905	1.921	1.922
Case-3 ($k_h = 0.08$)	1.511	1.562	1.513	1.564	1.613	1.648
Case-4 ($k_h = 0.08$)	1.316	1.401	1.318	1.403	1.329	1.401
Case-5 ($k_h = 0.16$)	1.083	1.139	1.087	1.141	1.133	1.181
Case-6 ($k_h = 0.16$)	1.002	1.099	1.005	1.102	1.005	1.091

shear strength of potential failure mass as a whole for the two slope sections at CH 21.00 and CH 22.00 respectively.

Effect of Drawdown on Seismic FOS

For Horizontal Seismic Coefficient k_h = 0.08

The analyses are carried out considering horizontal seismic coefficient k_h value as 0.08. The seepage conditions are exactly similar to Case-1 and Case-2. Here also, Fig. 19 will represent the variation of pore-pressure at CH 21.00 and CH 22.00. For Case-3, FOS value for upstream slope stability analysis at CH 21.00 is 1.511 whereas, FOS value at CH 22.00 is found out to be equal to 1.562. For Case-4, FOS value at CH 21.00 decreases considerably by 28.0% to 1.088 just after 10 days of drawdown (i.e. water level in the reservoir is at dead storage level). Then the FOS value slowly recovers with time by 15.1% as the excess pore-pressure dissipates and increases to 1.316 after 57 days. Whereas, a similar behavior in FOS value during the drawdown process is observed for slope at CH 22.00 with an initial decrease in FOS value by 26.2% to 1.153 just after 10 days of drawdown and final appreciation of the FOS value by 15.9% to 1.401 after 57 days.

Figure 21 shows the variation in the FOS with time during and after drawdown for the two slope sections at CH 21.00 and CH 22.00 respectively. Similar conclusions like Case-1 and Case-2 regarding the initial decrease in FOS during the period of 10 days and then improvement of the FOS with passage of time against slope failure for slope at CH 21.00 and slope at CH 22.00 may also be drawn for these cases. Figure 22 shows the improvement in shear strength associated with each individual slice after the period of 57 days for both slope sections at CH 21.00 and CH 22.00 respectively.

Effect of Drawdown on Seismic FOS

For Horizontal Seismic Coefficient k_h = 0.16

For Case-5, FOS values for upstream slope stability analysis at CH 21.00 and CH 22.00 are observed as 1.083 and 1.139 respectively. For Case-6, there is significant reduction in FOS value at CH 21.00 by 23.9% to 0.824 just after 10 days of drawdown (i.e. water level in the reservoir is at dead storage level). However, as pore water pressure dissipates, it later improves by 16.4% to 1.002 after 57 days. Whereas, a similar behavior in FOS value during the drawdown process is observed for slope at CH 22.00 with initial decrease in FOS value by 21.2% to 0.898 just after 10 days of drawdown and final recovery by 16.8% to 1.099 after 57 days. In these cases also, the seepage conditions are similar to Case-1 and Case-2 respectively and therefore, the pore pressure variation will be similar as represented by Fig. 19 for two slopes at CH 21.00 and CH 22.00.

Figure 23 shows the variation in the FOS with time during and after drawdown for the two slope sections at CH 21.00 and CH 22.00 respectively. It is observed that if the horizontal seismic coefficient k_h is chosen as 0.16, then the FOS value decreases below unity after the drawdown starts and again recovers with passage of time. These results indicate that if an earthquake of such nature occurs during drawdown process, it may lead to failure of the embankment. Furthermore, Fig. 24 shows improvement in shear strength associated with each individual slice after the completion of 57 days.

Effect of Seismic Acceleration on Static FOS, Shear Strength and Mobilized Shear

For Constant Reservoir, Water Level (i.e. Steady Seepage-State)

Table 6 presents the percentage change in FOS value of upstream slope for Case-3 and Case-5 with respect to that of Case-1.

Figure 25 shows the effect of horizontal acceleration on shear strength profile for slope section at CH 21.00 and CH 22.00 respectively. The comparisons are made for Case-1, Case-3 and Case-5 respectively. In all these three cases, the seepage conditions are similar (i.e. steady state seepage condition). The effect of the horizontal seismic acceleration on shear strength as well as on mobilized shear has

been compared for different cases. The decrease in shear strength under seismic load is governed the amount $(k_h W \mathrm{Sin}\alpha)$ as evident in Eq. (10). The application of seismic load has large influence on mobilized shear and magnitude of mobilized shear increased by $(k_h W \mathrm{Cos}\alpha)$ as expressed in Eq. (11). Figure 26 shows the effect of horizontal acceleration on mobilized shear profile for slope section at CH 21.00 and CH 22.00 respectively. It is observed that the mobilized shear is maximum for seismic analysis when $k_h = 0.16$ in comparison to the static Case-1.

Effect of Seismic Acceleration on Static FOS, Shear Strength and Mobilized Shear

For Drawdown in Reservoir Water Level (i.e. Transient-State Seepage).

Table 7 presents the percentage decrease in FOS value of upstream slope for Case-4 and Case-6 with respect to that of Case-2.

Figure 27 shows the effect of horizontal acceleration on shear strength. In addition, Fig. 28 shows effect of earthquake acceleration on mobilized shear for slope section at CH 21.00 and, CH 22.00 respectively. Here also, similar explanations regarding the variations of shear strength and mobilized shear along the slip surface are applicable as were given for Case-1, Case-3 and, Case-5.

From Tables 6 and 7, it is observed that the percentage decrease in FOS values differ significantly. These two tables reflect the percentage decrease in FOS under different horizontal seismic coefficient (k_h) for full reservoir level and at the end of 57 days respectively for the upstream slope. It is evident from Figs. 16 and 17 that the phreatic surface intersects the failure mass for both sections at CH 21.00 as well as CH 22.00. From Figs. 16 and 17, it can be seen that the effective weight of the failure mass as a whole is different for Case-1, Case-3 and Case-5 (i.e. under full reservoir level) to that of Case-2, Case-4 and Case-6 (i.e. at the end of 57 days). This is because of the change in phreatic surface intersecting the failure mass in these two scenarios. That is why, with each increment of horizontal seismic coefficient, the percentage decrease in FOS values estimated is quite different in Table 6 as compared to Table 7.

Conclusion

In this paper, a case study analysis on Durgawati earthen dam is presented. The upstream and downstream slopes of the earthen embankment have been analyzed for two sections namely CH 21.00 and CH 22.00 respectively. The slopes have been analyzed for steady state seepage and transient state seepage (to simulate reservoir drawdown condition). Also, the effect of seismic loading is considered in the form of pseudo-static analysis. Two values of horizontal seismic coefficient (k_h) have been considered in the analyses. The different analyses have been categorized as Case-1 to Case-6 and the following conclusions have been drawn from the present work:

1. The downstream slopes have been found to be safe for all cases because the FOS values are always greater than unity. It is found that when drawdown occurs, the FOS value increases with time at section CH 21.00. However, the FOS remains constant during drawdown process at section CH 22.00.
2. For upstream slope, under steady seepage condition (i.e. case-1, case-3 and case-5), the FOS value is always greater than unity indicating the slope is stable for static as well as for seismic loading condition. Under transient seepage condition (for case-2, case-4 and case-6), the FOS value initially decreases during first 10 days of drawdown process and then recovers. For case-2 and case-4, the FOS values never reduce below unity during whole drawdown process indicating the structure is safe. However, for case-6, it is observed that the FOS value becomes less than unity just after 3 days of the beginning of drawdown process and then slowly recovers. The FOS value remains below unity up to next 55 days. Therefore, the slope remains in a critical condition during this period. This phenomenon indicates that if an earthquake of similar magnitude (i.e. $k_h = 0.16$) occurs during drawdown process, the upstream slope at CH 21.00 and CH 22.00 may fail.
3. For downstream slope, it is observed that an earthquake event having $k_h = 0.08$ under steady seepage condition lowers the static FOS value by 20% at both

Table 6 Percentage decrease in factor of safety (FOS) for upstream slope

Embankment Dam conditions	FOS at CH 21.00	% Decrease in FOS	FOS at CH 22.00	% Decrease in FOS
Case-1	2.423	37.6%	2.423	35.5%
Case-3 ($k_h = 0.08$)	1.511		1.562	
Case-1	2.423	55.3%	2.423	53.0%
Case-5 ($k_h = 0.16$)	1.083		1.139	

Table 7 Percentage decrease in factor of safety (FOS) for upstream slope

Embankment Dam conditions	FOS at CH 21.00	% Decrease in FOS	FOS at CH 22.00	% Decrease in FOS
Case-2	1.875	29.8%	1.904	26.4%
Case-4 ($k_h = 0.08$)	1.316		1.401	
Case-2	1.875	46.6%	1.904	42.3%
Case-6 ($k_h = 0.16$)	1.002		1.099	

section CH 21.00 and CH 22.00. The decrease in static FOS value during transient seepage state is also about 20%. Moreover, an earthquake event of higher seismic coefficient (i.e. $k_h = 0.16$) results in reduction of static FOS value by 36% during both steady as well as transient seepage condition.

4. Similarly, for upstream slope, average reduction in FOS value at both section during steady seepage condition is about 36% of static FOS under seismic loading with $k_h = 0.08$, whereas average decrease in FOS is 28 about % of static FOS value during transient seepage condition under same seismic loading (i.e. $k_h = 0.08$) condition. Moreover, with higher seismic coefficient (i.e. $k_h = 0.16$), average decrease in static FOS value for both section is about 54% under steady seepage condition and about 44% under drawdown condition.
5. In overall, it is observed that the FOS value against slope failure decreases if earthquake loading is considered compared to the static condition. This reduction in static FOS with application of a seismic horizontal acceleration is mainly accomplished by increase in mobilized shear at base of each individual slice along the potential failure surface. However, a reduction in shear strength along the slice also occurs with application of seismic load but this reduction is lesser compared to the increase in mobilized shear. This is true for both slopes i.e. sections CH 21.00 and CH 22.00.
6. The seepage and slope stability analyses have been carried out based on the data of only two sections namely CH 21.0 and CH 22.0. In other sections along the length of the dam, if the dam profile and material parameters change, then calculations and results should change accordingly.

Acknowledgements The authors would like to express their indebtedness to Water Resource Department, Government of Bihar for supplying all the necessary data to perform this work.

References

1. SEEP/W (2005) Seepage analyses, Software permitted for limited period of use by GeoSlope Office, Canada. lorin@geo-slope.com
2. SLOPE/W (2002) Stability Analysis, Users guide version 5, GeoSlope Office, Canada. www.geoslope.com
3. Fellenius W (1936) Calculation of stability of earth dams. In: Proceedings of the second congress of large dams, vol 4, pp 445–463
4. Bishop AW (1955) The use of slip circle in the stability analysis of slopes. Geotechnique 5(1):7–17
5. Bishop AW, Morgenstern N (1960) Stability coefficients for earth slopes. Geotechnique 10(4):164–169
6. Janbu N (1954) Applications of composite slip surfaces for stability analyses. In: Proceedings of the European conference on the stability of earth slopes, Stockholm, vol 3, pp 39–43
7. Janbu N (1968) Slope stability computations. Soil mechanics and foundation engineering report. The Technical University of Norway, Trondheim, Norway
8. Morgenstern NR, Price VE (1965) The analysis of the stability of general slip surfaces. Geotechnique 15(1):79–93
9. Spencer E (1967) A method of analysis of the stability of embankments assuming parallel inter-slice forces. Geotechnique 17(1):11–26
10. Sarma SK (1973) Stability analysis of embankments and slopes. Geotechnique 23(3):423–433
11. Lowe J, Karafaith L (1960) Stability of earth dams upon draw down. In: Proceeding 1st Pan-Am conference soil mechanics and foundation engineering. Mexico City, vol 2, pp 537–552
12. Corps of Engineers (1970) Slope stability manual. EM 1110-2-1902.Washington, DC, Department of the Army office of the chief engineers
13. Fredlund DG, Krahn J (1977) Comparison of slope stability methods of analysis. Can Geotech J 14(3):429–439
14. Griffiths DV, Lane PA (1999) Slope stability analysis by finite elements. Geotechnique 49(3):387–403
15. Lane PA, Griffiths DV (2000) Assessment of stability of slopes under drawdown condition. J Geotechn Geo-environ Eng ASCE 126(5):443–450
16. Griffiths GV, Fenton GA (2004) Probabilistic slope stability analysis by finite elements. J Geotechn Geo-environ Eng ASCE 130(5):507–518
17. Zheng H, Sun G, Liu D (2009) A practical procedure for searching critical slip surfaces of slopes based on strength reduction technique. Comput Geotechn 36(1–2):1–5
18. Goh ATC (1999) Genetic algorithm based slope stability analysis using sliding wedge method. Can Geotechn J 36:382–391
19. Goh ATC (2000) Search for critical slip circle using genetic algorithms. J Civil Eng Environ Syst 17(3):181–211
20. McCombie PF, Wilkinson P (2002) The use of simple genetic algorithm in finding the critical factor of safety in slope stability analysis. Comput Geotechn 29:699–714
21. Sabhahit N, Sreeja J, Madhav MR (2002) Genetic algorithm for searching critical slip surface. Indian Geotechn J 32(2):86–101
22. Zolfaghari AR, Heath AC, McCombie PF (2005) Simple genetic algorithm search for critical non circular failure surface in slope stability analysis. Comput Geotechn 32:139–152

23. Bhattacharya RK, Satish MG (2007) Optimal design of a stable trapezoidal section using hybrid optimization techniques. J Irrig Drain Eng ASCE 1333(4):323–329
24. Cheng YM, Liang L, Chi SC, Wei WB (2007) Particle swarm optimization algorithm for location of the critical non circular failure surface in two-dimensional slope stability analysis. Comput Geotechn 34:92–103
25. Nagesh Kumar D, Janga Reddy M (2007) Multipurpose reservoir operation using particle swarm optimization. J Water Resourc Plann Manag ASCE 133(3):192–201
26. Sivakugan N, Das BM (2009) Geotechnical engineering: a practical problem solving approach. J. Ross Publishing, Plantation
27. Childs EC, Collis George N (1950) The permeability of porous materials. Proc R Soc 201:392–405
28. Richards LA (1931) Capillary conduction of liquids through porous mediums. J Appl Phys 1:318
29. Segerlind LJ (1984) Applied finite element analysis. Wiley, New York
30. IS: 1893 (1984) Indian standard criteria for earthquake resistant design of structures. Reaffirmed 2003 (Fourth revision). Bureau of Indian Standard (BIS). New Delhi, India
31. IS: 1893 (2002) Indian standards criteria for earthquake resistant design of structures, part-1. Bureau of Indian Standard (BIS). New Delhi, India
32. Hynes Griffin ME, Franklin AG (1984) Rationalizing the seismic coefficient method. US Army Corps of Engineers waterways experiment station, Vicksburg, Mississippi. Miscellaneous Paper GL 84-13:21
33. Chakraborty D, Choudhury D (2009) Investigation of the behavior of tailings earthen dam under seismic conditions. Am J Eng Appl Sci 2(3):559–564
34. A design report on Durgawati Reservoir project, Earthen dam section at RD 640.09 (CH-21.00) & RD 670.57 (CH-22.00). Central water commission Govt of India. DRG NO: DIG-1050-C-2357, FILE. NO. 2/14/2001-EMB (N&W)